



HAL
open science

Multi-Antenna Wireless Powered Relaying: Low Complexity and Near Optimal Techniques for Generic EH Models

George Ropokis, Petros Bithas

► **To cite this version:**

George Ropokis, Petros Bithas. Multi-Antenna Wireless Powered Relaying: Low Complexity and Near Optimal Techniques for Generic EH Models. *IEEE Transactions on Green Communications and Networking*, 2024, 10.1109/TGCN.2023.3343186 . hal-04467415

HAL Id: hal-04467415

<https://univ-rennes.hal.science/hal-04467415>

Submitted on 25 Apr 2024

HAL is a multi-disciplinary open access archive for the deposit and dissemination of scientific research documents, whether they are published or not. The documents may come from teaching and research institutions in France or abroad, or from public or private research centers.

L'archive ouverte pluridisciplinaire **HAL**, est destinée au dépôt et à la diffusion de documents scientifiques de niveau recherche, publiés ou non, émanant des établissements d'enseignement et de recherche français ou étrangers, des laboratoires publics ou privés.



Distributed under a Creative Commons Attribution - NonCommercial 4.0 International License

Multi-Antenna Wireless Powered Relaying: Low Complexity and Near Optimal Techniques for Generic EH Models

George A. Ropokis and Petros S. Bithas

Abstract—We investigate Wireless Powered Multi-Relay Networks (WPRNs) equipped with multiple antennas both at the Source and the Relay and propose two different communication schemes. These schemes are based on the combination of Time Switching (TS) and Self-Energy Recycling (SER) and extend existing ones that have been developed for single-antenna sources. Following that, by adopting only the very generic assumption that the Energy Harvesting Model (EHM) is described by any non-decreasing function, we focus on the instantaneous rate maximization problem and design near-optimal beamforming and wireless power transfer-time determination algorithms for our schemes. A common characteristic of the presented algorithms is their low complexity and implementation simplicity. Given the generality of our EHM assumptions, our algorithms are applicable for all popular EHMs found in the literature, which are normally described using non-decreasing functions, without being specific to any of them. Various simulation results are presented that allow to evaluate the two schemes and compare them with existing benchmarks for different popular EHMs and relay availability scenarios. Finally, we bound the suboptimality of our solutions and verify their near-optimal performance for different EHMs.

Index Terms—Energy harvesting model-agnostic optimization, multi-antenna relays, self-energy recycling, simultaneous wireless information and power transfer, wireless powered relay networks.

I. INTRODUCTION

ENERGY Harvesting (EH) and Simultaneous Wireless Information and Power Transfer (SWIPT) have been recognized as promising technologies for supporting power-limited nodes and enabling a plethora of smart use cases in green 6G networks [1]–[3]. Moreover, the fact that SWIPT combines information transmission and Wireless Power Transfer (WPT), has lead to an immense interest on the design of SWIPT techniques and their application in a variety of communications systems, including also Wireless Powered Relaying (WPR) systems, i.e., systems where energy-constrained EH relays are employed in order to assist communication [4], [5]. In the recent years, Power Splitting (PS) and Time Splitting (TS) protocols have been introduced for optimizing WPR-based networks. Among others, related works consider optimal multi-antenna designs [6], optimal resource allocation

in WPR-based multi-user systems [4], and optimal relay selection schemes [7], [8]. However, to the best of our knowledge, a common limitation in all these performance optimization efforts (as well as, in all related technical literature) is that they have as a starting point the adoption of some particular Energy Harvesting Model (EHM). As a result, the optimization solutions and algorithms presented in these works, are tied to the EHMs that they consider. Such an approach leads to EHM-specific results and thus restricts the applicability of existing analysis and system designs, to the EH circuit characteristics and/or the operating frequency bands which are identical (or close to) the ones used for the creation of the considered EHM. To tackle this weakness, in this paper, for the first time, we introduce an optimization framework for the design of WPR techniques which is agnostic to the considered EHM, i.e., it does not make any assumption about the form of the mathematical function describing the EH process, other than that it is a non-decreasing function.

A. Related Works

In the technical literature, several EHMs have been proposed in order to model non-linear EH characteristics, using specific families of parametric, non-linear, non decreasing functions (e.g., [9]–[11]), or piece-wise linear, non decreasing models [12]–[14]. Focusing on WPRs and Wireless Powered Relay Networks (WPRNs), several works consider WPRs with such non-linear EHMs, e.g., [15]–[19] and references therein. However, the majority of the works, is based on PS and TS WPT. As an alternative, Self-Energy Recycling (SER) WPRs have also been studied, (e.g., [12], [20], [21] and references therein) where the WPRs use different antennas for data transmission/reception and EH, and as a result, they are able to harvest energy while transmitting/receiving data. Moreover, schemes combining SER with TS and PS have been proven to deliver significant performance benefits for linear [22]–[24] and specific non-linear EHMs [14], [25]. In more detail, in [25], the problem of optimizing the WPR beamformer such as to maximize the signal-to-interference plus noise ratio (SINR) is treated. To this end, a single-relay decode and forward WPR with PS and SER is considered. More importantly, in [14], a wireless powered amplify-and-forward (AF) relaying communication scenario was investigated, in which relay selection was combined with TS, antenna switching, and SER. The scenario in [14] was the first to combine TS and SER and the results presented therein illustrated that such a combination

G. A. Ropokis is with CentraleSupélec, Campus Rennes, 35510, Cesson Sevigne, France and the Institute of Electronics and Telecommunication of Rennes, France (e-mail:georgios.ropokis@centralesupelec.fr).

P. S. Bithas is with the Department of Digital Industry Technologies, National and Kapodistrian University of Athens, Psahna, 34400, Greece (e-mail: pbithas@dind.uoa.gr).

is promising in terms of achieving higher rates in WPRNs. However, the algorithms of [14] are limited to systems with a single-antenna source. Moreover, the applicability of the results of all the above works is again limited due to the fact that they are based on specific EHM.

B. Motivation and Contributions

Motivated by the above and aiming to introduce new EH-agnostic communications models that will maximize the benefits of the combined use of TS and SER, in this work, we introduce two different TS/SER based transmission schemes. These schemes, unlike all previous works on WPRs and WPRNs, are EHM-agnostic, while also consider multiple antennas at both the source and the AF WPRs of the network. Further explaining the term EHM-agnostic, we use it to state that the only assumption that we make in our algorithmic design is that the relation between the input power to the EH circuits and the harvested power is described by a non-decreasing function. Finally, for the two schemes under consideration, we focus on the rate-optimal design problem and present near-optimal, low complexity algorithmic solutions for the problem of rate-optimal WPT time duration, and beamforming (BF) both at the source and the relays of the WPRN. In more detail, our contribution is highlighted as follows:

Our contributions: 1) We propose two new communications schemes that exploit multi-antenna relays in WPRNs, and combine SER with TS WPT. 2) We propose suboptimal, low complexity algorithms for optimizing the WPT time duration and the beamformers to be used at the source and the relays for both schemes. The optimization criterion used is the maximization of the instantaneous transmission rate. Our BF techniques avoid iterative, sophisticated optimization methods and only involve low dimensional optimization problems, for which we construct closed-form solutions. 3) Unlike existing works, we make no assumption for the EHM (other than that it is described by a non-decreasing function). As a result, our algorithms can be applied to all popular EHMs, which satisfy this property. 4) For each scheme, we derive upper bounds on their optimal rate. By comparing these bounds with our algorithmic solutions, it is shown that near-optimal performance is achieved with low complexity. Moreover, we also compare the rate performance of our algorithmic solutions with that of existing benchmarks and observe the superiority of our solutions with respect to traditional TS and PS based WPRNs.

Paper structure: In Section II, we introduce our system model and our novel communications schemes. In Sections III-IV we describe in detail our schemes and our methodology for optimizing their parameters. Furthermore, in Section IV, we also discuss several aspects related to the practical use of our schemes. In Section V, with the aid of extensive simulations, we evaluate the performance of the two schemes and compare it to that of existing benchmarks. Finally, Section VI, summarizes our findings.

Notation: Bold lower case letters denote vectors and bold upper case letters denote matrices. Operator $(\cdot)^H$ stands for the hermitian transpose of a vector/matrix and $\|\cdot\|$ for the

euclidean norm. Notation $\mathbf{h}^{(i)}$ denotes the i -th element of \mathbf{h} and $\mathbf{A}(m, \cdot)$ the m -th row of \mathbf{A} . Vector $\mathbf{h}^{\setminus m}$ is the vector created by eliminating the m -th element of \mathbf{h} , and $\mathbf{A}^{\setminus m}$ is the matrix created by eliminating the m -th row from \mathbf{A} . The identity matrix is expressed as \mathbf{I} , and $\lambda_{\min}(\mathbf{H})$ and $\lambda_{\max}(\mathbf{H})$ denote respectively the smallest and largest eigenvalue of hermitian matrix \mathbf{H} . Notation $\mathbf{H} \succeq 0$ indicates that \mathbf{H} is positive semidefinite. Operators $\text{rank}(\cdot)$ and $\text{tr}(\cdot)$ correspond to the rank and trace of a matrix respectively. Notation $\mathbf{w} \sim \mathcal{CN}(\mathbf{0}, \mathbf{R})$ denotes that \mathbf{w} follows a zero mean complex Gaussian distribution with covariance matrix \mathbf{R} . $\mathbb{E}\{\cdot\}$ denotes expectation.

II. SYSTEM MODEL

We study a system where a source S , equipped with M_S antennas, communicates with a single-antenna destination D with the help of L AF relays, denoted as $R_l, l = 1, \dots, L$. We set the number of antennas M_R at the relays to be greater than one, i.e., equal to $M_R = M + 1$, where $M \geq 1$. As in [12], [20], [21], [26], we assume that each relay has only one rectifier. Therefore, at any time instance, only one antenna can be used for EH purposes. We use the slotted communication protocol proposed in [12], where communication takes place in Time Frames (TFs), each one having a duration of T seconds. The protocol structure is explained in Table I, where it can be seen that each TF is split in three phases. Phase I constitutes the WPT subframe and phases II and III constitute the data transmission (DT) subframe. During phase I, all relays apply EH. However, during phases II and III, one of the relays, the one that can achieve the highest transmit rate for the specific TF, assists the communication of S and D , whereas the remaining relays apply EH. In what follows, we describe the WPT and the DT subframes, focusing mostly on the relay that is selected to assist communication during the considered TF. We denote this relay as R_{l^*} .

A. The Wireless Power Transfer Subframe

To discuss the WPT subframe, we first describe the characteristics that an EHM should satisfy such as to be compatible with our algorithmic solutions which we will propose in later sections.

1) *The considered EHMs:* We model the relation between the power P_{out} at the output of the EH circuit, and the power P_{in} at its input, as a function $P_h(\cdot)$, and express P_{out} as:

$$P_{out} = P_h(P_{in}), \quad (1)$$

where we make no assumption for $P_h(\cdot)$ other than that it is a non decreasing function of P_{in} . All popular EHMs which are normally adopted in the open technical literature satisfy this assumption, and our algorithms will be applicable for them. The operation during the WPT subframe is then summarized as follows.

2) *Source and relay operation during the WPT subframe:* The WPT subframe includes phase I, which has a duration of θT seconds, $\theta \in [0, 1)$. During phase I, S transmits an

TABLE I: The system model and the transmission schemes.

Energy Transmission Subframe (duration θT seconds)		
Phase I: Wireless Power Transfer Phase		
S transmits an energy bearing signal used for EH at all relays		
Data Transmission Subframe (duration $(1 - \theta)T$ seconds)		
Phase II	RHtTH scheme	Phase III
S transmits a data signal.	R receives it and processes it for communications purposes using $M = M_R - 1$ antennas. R uses remaining antenna to apply EH.	R forwards the signal received during phase II, using the same $M_R - 1$ antennas. R uses remaining antenna to apply EH.
RHtT scheme		
Same as RHtTH		R (using all its antennas) forwards the signal received during phase II.

energy signal x_e , and the signal at the m -th antenna of relay $R_l, l = 1, \dots, L$, is written as:

$$y_{r,l,1} = \mathbf{H}_{sr,l}(m, :) \mathbf{f}_1 \sqrt{P_s} x_e + \mathbf{n}_{r,l,1}(m), \quad (2)$$

where $\mathbf{H}_{sr,l}$ the $M_R \times M_S$ channel matrix, \mathbf{f}_1 the BF vector of S , and $\mathbf{n}_{r,l,1}$ the Additive White Gaussian Noise (AWGN) at the m -th antenna, characterized by a variance σ^2 . Assuming that the average power of signal x_e is equal to 1, i.e., $\mathbb{E}\{|x_e|^2\} = 1$, and that $\|\mathbf{f}_1\|^2 = 1$, S transmits using a power level P_s . The power of $y_{r,l,1}$ is then written as¹:

$$P_{in,l,1} = \mathbb{E}\{|y_{r,l,1}|^2\} = |\mathbf{H}_{sr,l}(m, :)\mathbf{f}_1|^2 P_s + \sigma^2 \quad (3)$$

$$\approx |\mathbf{H}_{sr,l}(m, :)\mathbf{f}_1|^2 P_s.$$

Focusing on R_{l^*} , in this work, we select \mathbf{f}_1 such as to maximize the energy harvested by R_{l^*} . Therefore, assuming that the $m_{l^*,1}$ -th antenna is used for EH at R_{l^*} during phase I, the optimal \mathbf{f}_1 is the Maximum Ratio Transmission (MRT) beamformer $\mathbf{f}_1 = \frac{\mathbf{H}_{sr,l^*}(m_{l^*,1}, :)^H}{\|\mathbf{H}_{sr,l^*}(m_{l^*,1}, :)\|}$, and the optimal $m_{l^*,1}$ is equal to $\arg \max \left\{ \|\mathbf{H}_{sr,l}(m, :)\|^2 \right\}$. The harvested energy at R_{l^*} is then equal to:

$$e_{h,l^*,1} = \theta T P_h \left(\max \left\{ \|\mathbf{H}_{sr,l}(m, :)\|^2 P_s \right\} \right). \quad (4)$$

B. The Data Transmission Subframe

Phases II and III comprise the DT subframe. During these two phases, R_{l^*} assists communication and the remaining relays apply EH. For the operation of R_{l^*} , we introduce the communication schemes of Table I (where RHtTH stands for Receive and Harvest then Transmit and Harvest and RHtT for Receive and Harvest then Transmit). We also describe the two schemes in more detail, in what follows.

RHtTH: This novel scheme exploits ideas initially proposed in [14] while also introducing two significant novelties. First, unlike [14], RHtTH considers a multi-antenna S . Second, unlike [14] where a piecewise linear $P_h(\cdot)$ is used, RHtTH only assumes that $P_h(\cdot)$ is a non decreasing function. Hence, RHtTH is fundamentally different of our prior work in [14]. We further describe RHtTH in Section III, where we also present our approach for optimizing its parameters.

¹In (3), we approximate the average power of $y_{r,l,1}$ by ignoring the contribution of noise to EH. This is a common approach in the technical literature and it is also adopted all throughout this paper.

RHtT: RHtT is based on receiving data and energy (during phase II) and forwarding data during phase III. Optimizing RHtT requires novel methods, that account for the multiple antennas at S and are suitable for the considered general EHM. RHtT is discussed in Section III-D.

C. Energy Consumption Characteristics and Constraints

We first discuss the energy consumption characteristics of the considered schemes.

1) *Energy consumption characteristics:* We use the power consumption model presented in [12], [14]. According to it, the power consumption of R_{l^*} during a TF (assuming that no power is consumed during the WPT phase) is given as:

$$E_{cons} = \frac{(1 - \theta)T}{2} \left(\frac{P_r}{\varepsilon} + P_C \right), \quad (5)$$

with

$$P_C = \begin{cases} P_C^{(RHtT)} = M_R P_{t_x} + (M_R - 1) P_{r_x} + 2P_C, & \text{for RHtT,} \\ P_C^{(RHtTH)} = (M_R - 1) (P_{t_x} + P_{r_x}) + 2P_C, & \text{for RHtTH,} \end{cases}$$

where P_r is the transmit power, $\varepsilon < 1$ the efficiency of the amplifiers associated with each one of the transmit antennas, and P_C the power consumption of the electronics of the data transmitting and the data receiving antennas of R_{l^*} , during phases III and II respectively. Using the power consumption model of [12], [14], and the description of RHtTH and RHtT, P_C this is found equal to the values given in (5), where P_{t_x} and P_{r_x} stand for the power consumption of the transmit and receive circuits attached to each of the relay antennas, and P_C for the power consumption of the remaining circuits of the relay which are not associated to neither the transmit nor the receive antennas².

2) *Energy consumption constraints:* In order to describe the energy consumption constraints for a given TF, we introduce parameters $E_l^{(start)}$ and $E_l^{(0)}$, where the first one is the energy available at relay R_l at the beginning of the considered TF and the second one is the energy available at R_l before the first TF, i.e., before the start of cooperation. Following then the design introduced in [12], [14], we assume that the system operates respecting the following constraints.

Energy preservation constraint: This constraint, proposed in [14], imposes that the power level P_r at R_{l^*} , should be selected such that the energy available at R_{l^*} at the end of the considered TF, is at least equal to the amount of energy $E_{l^*}^{(0)}$ available to it at the beginning of transmission.

²In later sections, e_{s,l^*} in (6), will be substituted by variable $e_{s,l^*}^{(RHtTH)}$ for RHtTH and by $e_{s,l^*}^{(RHtT)}$, for RHtT.

Energy causality constraint: The energy consumed during a TF should be at most equal to the energy available at the battery at the end of phase II.

By denoting as $e_{h,l,i}, i \in \{1, 2, 3\}$ the energy harvested by R_l during the i -th phase and defining the energy surplus at the end of phase II [14] as:

$$e_{s,l^*} = E_{l^*}^{(start)} + e_{h,l^*,1} + e_{h,l^*,2} - E_{l^*}^{(0)}, \quad (6)$$

we can work as in [14] and express these two constraints using the following one: $E_{cons} \leq e_{s,l^*} + \min \{e_{h,l^*,3}, E_{l^*}^{(0)}\}$, which can be finally rewritten as:

$$P_r \leq \frac{2\epsilon e_{s,l^*}}{(1-\theta)T} + \frac{2\epsilon \min \{e_{h,l^*,3}, E_{l^*}^{(0)}\}}{(1-\theta)T} - \epsilon PC. \quad (7)$$

Having introduced our schemes and their constraints, we discuss the rate optimization problem.

D. The Rate Optimal System Design Problem

In this work, we focus on maximizing the transmit rate of RHtTH and RHtT during a TF, subject to the combined energy preservation and energy causality constraints. To this end, we express the transmit rate for a TF as:

$$R = \frac{(1-\theta)T \log_2(1 + \rho_{srd,l^*})}{2}, \quad (8)$$

where ρ_{srd,l^*} is the Signal to Noise Ratio (SNR) on the $S \rightarrow R_{l^*} \rightarrow D$ link for the considered scheme. The process of optimizing RHtTH and RHtT involves determining: 1) the value of parameter θ for both schemes, 2) the index m_{l^*} of the antenna which should be used for EH during phase II (for RHtTH and RHtT) and phase III (for RHtT), 3) the optimal beamformer to be used by S during phase II (for both RHtTH and RHtT), and 4) the optimal beamformer to be used by R_{l^*} during phase III by RHtTH. However, since parameter θ appears in both schemes, we have decided to investigate in a common manner the process of determining its value. Besides that, for fixed θ , optimizing the system design requires solving the optimal phase II BF problem for S (for both schemes) and the optimal phase III BF problem for R_{l^*} (in case of RHtTH), for all candidate m_{l^*} values, and then selecting the value of m_{l^*} , that results in maximizing the transmit rate. As a result, rate optimal system design requires solving the fundamental subproblems of 1) rate-optimal BF at S (during phase II) and R_{l^*} (during phase III) for RHtTH; 2) rate-optimal BF at S (during phase II) for RHtT for all candidate m_{l^*} . Therefore, in the following sections, we present in more detail the two schemes and discuss our approach for maximizing their rate (or equivalently their SNR in case of a fixed value of θ), for a fixed value of θ and a fixed EH antenna m_{l^*} . The problem of determining m_{l^*} and θ is then treated in Section IV.

III. THE RHTTH AND RHTT SCHEMES

In what follows, we describe phases II and III of RHtTH, focusing on R_{l^*} . We then highlight the differences in the system model and the optimization of RHtT, with respect to RHtTH.

A. Operation During Phase II

During phase II, S transmits a data signal x_d (where $\mathbb{E} \{|x_d|^2\} = 1$) using a unit-norm beamformer \mathbf{f}_2 and a power level P_s . Let $\tilde{\mathbf{H}}_{sr,l^*} = \mathbf{H}_{sr,l^*}^{\setminus m_{l^*}}$ be the $M \times M_S$ MIMO channel between the M_S antennas at S and the M data receiving antennas at R_{l^*} . The signal at the data receiving antennas of R_{l^*} is then written as:

$$\mathbf{y}_{r,l^*,2}^{(d)} = \tilde{\mathbf{H}}_{sr,l^*} \mathbf{f}_2 \sqrt{P_s} x_d + \mathbf{n}_{r,l^*,2}^{(d)}, \quad (9)$$

where $\mathbf{n}_{r,l^*,2}^{(d)} \sim \mathcal{CN}(\mathbf{0}, \sigma^2 \mathbf{I})$ the AWGN at R_{l^*} . Applying Maximum Ratio Combining (MRC), i.e., using the combiner $\mathbf{v} = \tilde{\mathbf{H}}_{sr,l^*} \mathbf{f}_2 / \|\tilde{\mathbf{H}}_{sr,l^*} \mathbf{f}_2\|$, at the output of these antennas (such as to maximize the $S \rightarrow R_{l^*}$ SNR), we can express the SNR at the output of the combiner as:

$$\rho_{sr,l^*}^{(RHtT)} = \frac{G_{sr,l^*} P_s}{\sigma^2}, \quad (10)$$

where $G_{sr,l^*} = \mathbf{f}_2^H \tilde{\mathbf{H}} \mathbf{f}_2$, with $\tilde{\mathbf{H}} = \tilde{\mathbf{H}}_{sr,l^*}^H \tilde{\mathbf{H}}_{sr,l^*}$. Concerning the EH process at R_{l^*} , using the channel $\hat{\mathbf{h}}_{sr,l^*} = \mathbf{H}_{sr,l^*}(m_{l^*}, :)$, which is formed between S and the EH antenna of R_{l^*} , we can write the signal used for EH as:

$$y_{r,l^*,2}^{(h)} = \hat{\mathbf{h}}_{sr,l^*} \mathbf{f}_2 \sqrt{P_s} x_d + n_{r,l^*,2}^{(h)}, \quad (11)$$

where $n_{r,l^*,2}^{(h)} \sim \mathcal{CN}(0, \sigma^2)$ the AWGN at the EH antenna. The harvested energy at $R_{l^*}^*$ during phase II is then given as:

$$\begin{aligned} e_{h,l^*,2}^{(RHtT)} \left(\mathbf{f}_2^H \hat{\mathbf{H}} \mathbf{f}_2 \right) &= \frac{(1-\theta)T}{2} \mathbb{E} \left\{ \left| y_{r,l^*,2}^{(h)} \right|^2 \right\} \\ &\approx \frac{(1-\theta)T}{2} P_h \left(\mathbf{f}_2^H \hat{\mathbf{H}} \mathbf{f}_2 P_s \right), \text{ with } \hat{\mathbf{H}} = \hat{\mathbf{h}}_{sr,l^*}^H \hat{\mathbf{h}}_{sr,l^*}. \end{aligned} \quad (12)$$

B. Phase III: Data Transmission/EH from/at R

During phase III, R_{l^*} amplifies and forwards $y_{r,l^*,2}$ to D using all antennas except for antenna m_{l^*} , which is going to be used for EH. The signal reaching D is then expressed as

$$y_d = \frac{\tilde{\mathbf{h}}_{rd,l^*} \mathbf{x} y_{r,l^*,2}^{(d)}}{\sqrt{G_{sr,l^*} P_s + \sigma^2}} + n_{d,3}, \text{ with } \tilde{\mathbf{h}}_{rd,l^*} = \mathbf{h}_{rd,l^*}^{\setminus m_{l^*}}, \quad (13)$$

where $\mathbf{x} \in \mathbb{C}^{M \times 1}$ is the BF vector applied by R_{l^*} , and $y_{r,l^*,2}^{(d)}$ the signal at R_{l^*} 's combiner output.

Concerning the EH process, working as in [12], [14], we can show that by selecting the signal transmitted by S to be of the form $x_d e^{j\psi}$, with ψ set such that $\arg(\hat{\mathbf{h}}_{sr,l^*} \mathbf{f}_3 e^{j\psi}) = \arg(\mathbf{x}^H \mathbf{h}_{loop})$ and \mathbf{f}_3 set to be an MRT beamformer, the harvested energy is maximized and is equal to

$$\begin{aligned} e_{h,l^*,3}^{*(RHtTH)} \left(\mathbf{f}_2^H \tilde{\mathbf{H}} \mathbf{f}_2, \mathbf{x} \right) &= \frac{(1-\theta)T}{2} \\ &P_h \left(P_s \left(\|\hat{\mathbf{h}}_{sr}\| + \sqrt{\frac{\mathbf{f}_2^H \tilde{\mathbf{H}} \mathbf{f}_2 \|\mathbf{h}_{loop}\|^2}{\mathbf{f}_2^H \tilde{\mathbf{H}} \mathbf{f}_2 P_s + \sigma^2}} \right)^2 \right). \end{aligned} \quad (14)$$

Finally, using (4) and (12), we can express the RHtTH energy surplus as:

$$e_{s,l^*}^{(RHtTH)} \left(\mathbf{f}_2^H \hat{\mathbf{H}} \mathbf{f}_2 \right) = E_{l^*}^{(start)} + e_{h,l^*,1} + e_{h,l^*,2}^{(RHtTH)} \left(\mathbf{f}_2^H \hat{\mathbf{H}} \mathbf{f}_2 \right) - E_{l^*}^{(0)}. \quad (15)$$

The combined constraint introduced in (7) is then written as:

$$\|\mathbf{x}\|^2 \leq \frac{2\varepsilon \min \left\{ e_{h,l^*,3}^{*(RHtTH)} \left(\mathbf{f}_2^H \tilde{\mathbf{H}} \mathbf{f}_2, \mathbf{x} \right), E_{l^*}^{(0)} \right\}}{(1-\theta)T} + \frac{2\varepsilon e_{s,l^*}^{(RHtTH)} \left(\mathbf{f}_2^H \hat{\mathbf{H}} \mathbf{f}_2 \right)}{(1-\theta)T} - \varepsilon P_C^{(RHtTH)}. \quad (16)$$

C. The Process of Optimizing the RHtTH Scheme

In what follows, we present our approach for optimizing RHtTH. This approach greatly extends the solutions presented in [14] that merely consider a single-antenna S and a simple piecewise linear EHM. We start the presentation of this process by assuming predetermined values for θ and m_{l^*} , we focus on determining \mathbf{f}_2 and \mathbf{x} such as to maximize the instantaneous rate or equivalently the instantaneous SNR. To solve this problem, we notice that the $S \rightarrow R_{l^*}$ channel is the equivalent of a Single Input Single Output (SISO) channel having an SNR equal to $\rho_{sr,l^*}^{(RHtTH)} = \frac{G_{sr,l^*} P_s}{\sigma^2}$, and that (from (13)) the $R_{l^*} \rightarrow D$ SNR is equal to: $\rho_{rd,l^*}^{(RHtTH)} = \frac{|\mathbf{x}^H \tilde{\mathbf{h}}_{rd,l^*}|^2}{\sigma^2}$. The problem of the $S \rightarrow R_{l^*} \rightarrow D$ SNR maximization (denoted as ρ_{srd,l^*}) is then expressed as

$$\begin{aligned} \text{maximize}_{\mathbf{f}_2, \mathbf{x}}: & \rho_{srd,l^*}^{(RHtTH)} \frac{G_{sr,l^*} P_s |\tilde{\mathbf{h}}_{rd,l^*} \mathbf{x}|^2}{\sigma^2 \left(G_{sr,l^*} P_s + |\tilde{\mathbf{h}}_{rd,l^*} \mathbf{x}|^2 + \sigma^2 \right)} \\ \text{s.t.}: & \|\mathbf{f}_2\|^2 = 1, \text{ and (16)}. \end{aligned} \quad (P1)$$

To tackle (P1) we first introduce the following theorem.

Theorem 1: For RHtTH, for any vector \mathbf{f}_2 , a corresponding optimal relay beamformer \mathbf{x} for R_{l^*} can be found in the form:

$$\begin{aligned} \mathbf{x} &= \gamma_1 e^{j\phi_1} \mathbf{u}_1 + \gamma_2 e^{j\phi_2} \mathbf{u}_2, \text{ where } \mathbf{u}_1 = \left(\frac{\mathbf{h}_{loop}}{\|\mathbf{h}_{loop}\|} \right)^H, \\ \mathbf{u}_2 &= \frac{(\mathbf{I} - \mathbf{u}_1 \mathbf{u}_1^H) \tilde{\mathbf{h}}_{rd,l^*}^H}{\left\| (\mathbf{I} - \mathbf{u}_1 \mathbf{u}_1^H) \tilde{\mathbf{h}}_{rd,l^*}^H \right\|}, \end{aligned} \quad (17)$$

with $\phi_i \in [0, 2\pi), i \in \{1, 2\}$, selected such that: $\arg \left(e^{j\phi_1} \tilde{\mathbf{h}}_{rd,l^*} \mathbf{u}_1 \right) = \arg \left(e^{j\phi_2} \tilde{\mathbf{h}}_{rd,l^*} \mathbf{u}_2 \right)$, and $\gamma_1, \gamma_2 \in \mathbb{R}^+$ found by solving the problem:

$$\begin{aligned} \text{maximize}_{\gamma_1 \in \mathbb{R}^+, \gamma_2 \in \mathbb{R}^+}: & \alpha\gamma_1 + \beta\gamma_2 \\ \text{s.t.}: & \gamma_1^2 + \gamma_2^2 \leq \frac{2\varepsilon \min \left\{ e_{h,l^*,3}^{(opt)} \left(\mathbf{f}_2^H \tilde{\mathbf{H}} \mathbf{f}_2, \gamma_1 \right), E_{l^*}^{(0)} \right\}}{(1-\theta)T} \\ & + \frac{2\varepsilon e_{s,l^*}^{(RHtTH)} \left(\mathbf{f}_2^H \hat{\mathbf{H}} \mathbf{f}_2 \right)}{(1-\theta)T} - \varepsilon P_C^{(RHtTH)}, \end{aligned} \quad (C2.1)$$

where

$$e_{h,l^*,3}^{(opt)}(x, \gamma_1) = \frac{(1-\theta)T}{2} P_h \left(P_{in,l^*,3}^{(opt)}(x, \gamma_1) \right),$$

$$\text{with } P_{in,l^*,3}^{(opt)}(x, \gamma_1) = P_s \left(\left\| \hat{\mathbf{h}}_{sr} \right\| + \sqrt{\frac{x\gamma_1^2 \|\mathbf{h}_{loop} \mathbf{u}_1\|^2}{xP_s + \sigma^2}} \right)^2. \quad (19)$$

Proof: The proof follows the steps of [12, Theorem 1]. ■

In what follows, building on Theorem 1, we first simplify the jointly-optimal BF design (at S and R_{l^*}) problem and propose an algorithm for solving it.

1) *Simplifying the jointly optimal BF problem:* Since, for any beamformer \mathbf{f}_2 , \mathbf{x} has the structure described by Theorem 1, the jointly optimal vectors \mathbf{f}_2 and \mathbf{x} are found by determining the jointly optimal decision variables $(\mathbf{f}_2, \gamma_1, \gamma_2)$. Problem (P1) is therefore rewritten as:

$$\begin{aligned} \text{maximize}_{\mathbf{f}_2, \gamma_1 \in \mathbb{R}^+, \gamma_2 \in \mathbb{R}^+}: & \rho_{srd,l^*}^{(RHtTH)} = \frac{1}{\sigma^2} \frac{\mathbf{f}_2^H \tilde{\mathbf{H}} \mathbf{f}_2 P_s (\alpha\gamma_1 + \beta\gamma_2)^2}{\mathbf{f}_2^H \tilde{\mathbf{H}} \mathbf{f}_2 P_s + (\alpha\gamma_1 + \beta\gamma_2)^2 + \sigma^2} \\ \text{s.t.}: & \|\mathbf{f}_2\|^2 = 1, \text{ and (C2.1)}. \end{aligned} \quad (P3)$$

To simplify (P3), we consider a modified version that comes by introducing the constraint: $\mathbf{f}_2^H \tilde{\mathbf{H}} \mathbf{f}_2 = c$, for some value of c . The resulting problem is then written as:

$$\begin{aligned} \text{maximize}_{\mathbf{f}_2, \gamma_1 \in \mathbb{R}^+, \gamma_2 \in \mathbb{R}^+}: & \rho_{srd,l^*}^{(RHtTH)} \text{ s.t.}: \text{(C2.1)}, \|\mathbf{f}_2\|^2 = 1, \mathbf{f}_2^H \tilde{\mathbf{H}} \mathbf{f}_2 = c. \end{aligned} \quad (P3.1)$$

The following theorem specifies the characteristics of an optimal solution to this problem.

Theorem 2: There exists an optimal solution $(\mathbf{f}_2^*, \gamma_1^*, \gamma_2^*)$ to (P3.1), for which \mathbf{f}_2 is found by solving the problem:

$$\text{maximize}_{\mathbf{f}_2}: \mathbf{f}_2^H \hat{\mathbf{H}} \mathbf{f}_2, \text{ s.t.}: \mathbf{f}_2^H \tilde{\mathbf{H}} \mathbf{f}_2 = c, \mathbf{f}_2^H \mathbf{f}_2 = 1, \quad (P4)$$

and γ_1^*, γ_2^* are obtained by solving (P2) for the resulting \mathbf{f}_2^* .

Proof: Let us assume an optimal solution $(\mathbf{f}_2', \gamma_1', \gamma_2')$ to (P3.1), where \mathbf{f}_2' is not a solution to (P4). It then holds that $(\mathbf{f}_2')^H \tilde{\mathbf{H}} \mathbf{f}_2' = q$, with $q \in [\lambda_{\min}(\tilde{\mathbf{H}}), Q^*(c)]$, where $Q^*(c)$ denotes the Utility Function (UF) value at an optimal solution of (P4). We now notice that the UFs of (P2) and (P3.1) are increasing functions of γ_2 . This means that for the given \mathbf{f}_2' and γ_1', γ_2' should take the highest possible feasible value, which is found when (C2.1) is active, i.e., when:

$$\begin{aligned} \gamma_1'^2 + \gamma_2'^2 &= \frac{2\varepsilon \left(e_{s,l^*}^{(RHtTH)}(q) + \min \left\{ e_{h,l^*,3}^{(opt)}(c, \gamma_1'), E_{l^*}^{(0)} \right\} \right)}{(1-\theta)T} \\ &- \varepsilon P_C^{(RHtTH)}. \end{aligned} \quad (22)$$

Let us now consider the point $(\mathbf{f}_2^*, \gamma_1', \gamma_2')$ where \mathbf{f}_2^* is a solution to (P4). The UF of (P4) for $\mathbf{f}_2 = \mathbf{f}_2^*$, is then equal to $\mathbf{f}_2^{*H} \hat{\mathbf{H}} \mathbf{f}_2^* = Q^*(c) > q$. Hence, given again that the UFs of (P2) and (P3.1) are increasing functions of γ_2 , for $(\mathbf{f}_2^*, \gamma_1', \gamma_2')$ to be an optimal solution it must hold that:

$$\begin{aligned} \gamma_1'^2 + \gamma_2'^2 &= \frac{2\varepsilon \left(e_{s,l^*}^{(RHtTH)}(Q^*(c)) + \min \left\{ e_{h,l^*,3}^{(opt)}(c, \gamma_1'), E_{l^*}^{(0)} \right\} \right)}{(1-\theta)T} \\ &- \varepsilon P_C^{(RHtTH)}. \end{aligned} \quad (23)$$

However, this is only possible only if $e_{s,l^*}^{(RHtTH)}(q) = e_{s,l^*}^{(RHtTH)}(Q^*(c))$ (which implies that γ_1', γ_2' is also a solution to (P2) for $\mathbf{f}_2 = \mathbf{f}_2^*$ and $(\mathbf{f}_2^*, \gamma_1', \gamma_2')$ satisfies the property

TABLE II: Complexity for calculating $\mathbf{z}_1, \mathbf{z}_2, A, B, C$ and solving (P6.1)

Operation	(\times)	($+$)	$\sqrt{\cdot}$	\tan^{-1}	cos	sin
Complexity of calculating $\mathbf{z}_1, \mathbf{z}_2, A, B, C$						
$\mathbf{z}_1 = \hat{\mathbf{h}}_{sr, l^*} / \ \hat{\mathbf{h}}_{sr, l^*}\ , \mathbf{p} = \mathbf{q} - (\mathbf{z}_1^H \mathbf{q}) \mathbf{z}_1, \mathbf{z}_2 = \mathbf{p} / \ \mathbf{p}\ $	$16M_S$	$12M_S - 4$	2	0	0	0
$\tilde{\mathbf{H}}\mathbf{z}_1, \mathbf{z}_1^H \tilde{\mathbf{H}}\mathbf{z}_1$ and $\mathbf{z}_2^H \tilde{\mathbf{H}}\mathbf{z}_1$ and $\mathbf{z}_2^H \tilde{\mathbf{H}}\mathbf{z}_2$	$8M_S^2 + 12M_S$	$8M_S^2 + 8M_S - 6$	0	0	0	0
Complexity analysis for solving (P6.1)						
Calculating variables which are independent of c						
$q_2 = (A - B)^2, q_3 = \omega_1, \text{ and } \omega_2 = \omega_1 + \pi$	1	2	0	1	0	0
$D_1, D_2 = -D_1, q_4 = D_1^2, (A - B)^2 + D_1^2 = q_4 + q_2$	4	2	0	0	1	1
Calculating roots of (28)						
$2(c - B)q_1 + q_4, (c - B)^2$ and discriminant sq. root	6	4	1	0	0	0
Calculating δ_1 candidates	3	2	0	0	0	0
Check (29) $\forall (\delta_1, \omega_i)$	12	12	4	0	0	0
Total complexity for each value of c	21	18	5	0	0	0

at the best case equal to $\mathcal{O}((2M_S)^{4.5} \log(\frac{1}{\varepsilon}))$, the following significant advantages of our approach become evident: 1) it avoids sophisticated iterative optimization methods, such as the interior point method that may be difficult to implement in real-time systems, 2) exploiting accurate deterministic, polynomial approximations for inverse trigonometric functions, such as the ones in [27], our approach avoids iterative numerical methods (required for example for calculating the inverse tangent function), 3) The complexity of our approach grows as a function of M_S^2 while in case that (P4) is optimally solved for each c_k , it grows as a function of $(2M_S)^{4.5}$. This results in significant complexity differences for large number of antennas at S . Finally, in later sections, we will see that these complexity advantages do not influence the rate performance. We now focus on (P2).

3) *Solving (P2)*: This problem can be solved by noticing that it is an instance of the problem:

$$\text{maximize: } \alpha\gamma_1 + \beta\gamma_2 \quad (\text{P7})$$

$$\text{s.t.: } \gamma_1^2 + \gamma_2^2 \leq f(\gamma_1) - \varepsilon P_C^{(RH+TH)}, \quad (\text{C7.1})$$

$$\text{with } f(\gamma_1) = \frac{2\varepsilon \min \left\{ e_{h, l^*}^{(opt)} \left(\mathbf{f}_2^H \tilde{\mathbf{H}} \mathbf{f}_2, \gamma_1 \right), E_{l^*}^{(0)} \right\}}{(1 - \theta) T} + \frac{2\varepsilon e_{s, l^*}^{(RH+TH)} \left(\mathbf{f}_2^H \hat{\mathbf{H}} \mathbf{f}_2 \right)}{(1 - \theta) T}. \quad (\text{30})$$

It is noted that (P7) is significantly more challenging than the beamforming problem at R_l^* in [14]. This is due to the fact that in [14], $P_h(\cdot)$ in (1) is a piecewise linear function and the proposed beamforming algorithm is based on this assumption. On the contrary, in this work, following an EHM-agnostic strategy, we only assume that $P_h(\cdot)$ in (1) and $f(\cdot)$ in (P7) are non-decreasing functions of their input arguments. The resulting algorithm is summarized in Algorithm 1, and it is based on generating multiple feasible points and selecting the one that results in the best UF value. Steps 1, \dots , K of this method are also described in detail in what follows.

Step 1 - Obtaining a first candidate point: Since $f(\gamma_1)$ is non decreasing, we can lower bound $f(\gamma_1)$ by $f(0)$ and obtain

Algorithm 1 Solving (P7)

Input: $\theta, m_{l^*}, \mathbf{H}_{sr}, \mathbf{h}_{rd}, E_{l^*}^{(start)}, K_c$

- 1: Step 1: Substitute $f(\cdot)$ in (P7) by a lower constant bound for its value and solve the resulting problem to obtain a feasible point $(\gamma_1^{(0)}, \gamma_2^{(0)})$ for (P7). Set the optimal one.
- 2: **for** $k = 1$ to K , **do**
- 3: Step k : Use $(\gamma_1^{(k-1)}, \gamma_2^{(k-1)})$ in order to create a new, tighter constant lower bound for $f(\cdot)$, which is applicable for $\gamma_1 \geq \gamma_1^{(k-1)}$, and solve the problem obtained by substituting $f(\cdot)$ by this bound, and also adding the constraint $\gamma_1 \geq \gamma_1^{(k-1)}$. If the new beamformer results in a higher value for the objective of (P7), set this beamformer as the optimal one.
- 4: **end for**
- 5: **return** γ_1, γ_2

feasible γ_1, γ_2 values by solving the problem:

$$\text{maximize: } \alpha\gamma_1 + \beta\gamma_2 \text{ s.t.: } \gamma_1^2 + \gamma_2^2 \leq f(0) - \varepsilon P_C, \quad (\text{P8})$$

as described in Appendix B. Let $\gamma_1^{(0)}$ be the optimal γ_1 value for (P8). The feasible value of γ_2 that maximizes the UF value of (P7) for $\gamma_1 = \gamma_1^{(0)}$ is obtained when (C7.1) is active, i.e., for:

$$\gamma_2 = \gamma_2^{(0)} = \sqrt{f(\gamma_1^{(0)}) - \varepsilon P_C - (\gamma_1^{(0)})^2}, \quad (\text{32})$$

and point $(\gamma_1^{(0)}, \gamma_2^{(0)})$ is a feasible point for (P7).

Step $k > 1$ - Constructing new candidate points: Assuming that $(\gamma_1^{(k-1)}, \gamma_2^{(k-1)})$ satisfies the condition:³

$$(\gamma_1^{(k-1)})^2 + (\gamma_2^{(k-1)})^2 = f((\gamma_1^{(k-1)})^2) - \varepsilon P_C, \quad (\text{33})$$

we can obtain additional feasible points for (P7) if we introduce the constraint $\gamma_1 \geq \gamma_1^{(k-1)}$. It is then evident that due to monotonicity of $f(\cdot)$, whenever $\gamma_1 \geq \gamma_1^{(k-1)}$ and constraint $\gamma_1^2 + \gamma_2^2 \leq f(\gamma_1, f) - \varepsilon P_C$ is satisfied, (C7.1) is also satisfied.

³It is easy to verify the validity of this assumption.

As a result, a feasible value $\gamma_1^{(k)}$ for γ_1 in (P7) is found by solving the problem:

$$\begin{aligned} & \underset{\gamma_1 \in \mathbb{R}^+, \gamma_2 \in \mathbb{R}^+}{\text{maximize:}} \quad \alpha\gamma_1 + \beta\gamma_2, \text{ s.t.: } \gamma_1 \geq \gamma_f, \\ & \gamma_1^2 + \gamma_2^2 \leq f(\gamma_{1,f}) - \varepsilon P_C, \end{aligned} \quad (\text{P8.1})$$

as explained in Appendix B. A feasible point $(\gamma_1^{(k)}, \gamma_2^{(k)})$ for (P7) is then obtained by setting

$$\gamma_2^{(k)} = \sqrt{f(\gamma_1^{(k)}) - \varepsilon P_C - (\gamma_1^{(k)})^2}. \quad (35)$$

Finally, using the analysis of Appendix B and assuming the generation of K_γ additional points, after the generation of $(\gamma_1^{(0)}, \gamma_2^{(0)})$, the complexity of our approach is equal to $7(K_\gamma + 1)$ multiplications, $4(K_\gamma + 1)$ additions and $2(K_\gamma + 1)$ square root calculations. Adding to this complexity the complexity of K_γ evaluations of $f(\gamma_{1,f})$ and K_γ additions (required in order to calculate the term $f(\gamma_{1,f}) - \varepsilon P_C$ at each one of the K_γ steps following the calculation of $(\gamma_1^{(0)}, \gamma_2^{(0)})$), the total complexity of generating the feasible solutions for (P2) is found. It is also observed that provided that the evaluation of function $f(\cdot)$, i.e., of $P_h(\cdot)$, is of reasonable computational cost⁴, the complexity of our approach for (P2) is limited.

4) *The final algorithm:* Combining our methods for solving (P4) and (P2), our algorithm for solving (P1) is summarized in Algorithm 2. Exploiting the complexity analyses for our approach for (P4) and (P2), the computational complexity of Algorithm 2 can be trivially calculated. Having presented the

Algorithm 2 Optimizing the relay beamformer for RHtTH

Input: $\theta, m_{l^*}, \mathbf{H}_{sr}, \mathbf{h}_{rd}, E_{l^*}^{(start)}, K_c$

- 1: Set the optimal SNR equal to $\rho = 0$, $\hat{\mathbf{h}}_{sr} = \mathbf{H}_{sr, l^*}(m_{l^*}^*, :)$ and $\tilde{\mathbf{H}}_{sr, l^*} = \mathbf{H}_{sr, l^*}^{\{m_{l^*}^*\}}$
- 2: Calculate $\hat{\mathbf{H}} = \hat{\mathbf{h}}_{sr, l^*}^H \mathbf{h}_{sr, l^*}$, $\tilde{\mathbf{H}} = \tilde{\mathbf{H}}_{sr, l^*} \tilde{\mathbf{H}}_{sr, l^*}$, $c_{min} = \lambda_{min}(\tilde{\mathbf{H}})$, and $c_{max} = \lambda_{max}(\tilde{\mathbf{H}})$
- 3: **for** $k = 0$ to K_c **do**
- 4: Set $c = c_{min} + \frac{k}{K_c}(c_{max} - c_{min})$ and suboptimally solve (P4) considering beamformers of the form (25) and Theorem 3 in order to determine a candidate beamformer $\mathbf{f}_{2,k}$ for S .
- 5: Calculate $Q = \mathbf{f}_{2,k}^H \hat{\mathbf{H}} \mathbf{f}_{2,k}$, set $\mathbf{f}_2^H \hat{\mathbf{H}} \mathbf{f}_2 = Q$ and solve (P2) to obtain values $\gamma_{1,k}$ and $\gamma_{2,k}$ for γ_1 and γ_2 .
- 6: If $\left(\rho_k = \frac{1}{\sigma^2} \frac{c P_s (\alpha\gamma_{1,k} + \beta\gamma_{2,k})^2}{c P_s + (\alpha\gamma_{1,k} + \beta\gamma_{2,k})^2 + \sigma^2} > \rho\right)$, set $\rho = \rho_k$, $\mathbf{f}_2 = \mathbf{f}_{2,k}$, $\gamma_1 = \gamma_{1,k}$, $\gamma_2 = \gamma_{2,k}$
- 7: **end for**
- 8: **return** $\rho, \mathbf{f}_2, \gamma_1, \gamma_2$

RHtTH and the process for optimizing it, we now discuss RHtT.

⁴For most popular EH models, $P_h(\cdot)$ is characterized by a small number of operations involving linear, low-order polynomial and/or exponential terms, which are considered functions of relatively low implementation cost.

D. The RHtT Scheme

1) *Operation During Phases II and III:* In case of RHtT, operation during phase II is identical to that of RHtTH, and the signal and SNR analysis of Section III-A is directly applicable. On the other hand, during phase III, R_l^* uses all its antennas to forward data to D , employing an MRT beamformer. The signal reaching D is therefore expressed as:

$$y_d = \frac{\mathbf{h}_{rd, l^*} \mathbf{x} y_{r, l^*}^{(d)}}{\sqrt{G_{sr, l^*} + \sigma^2}} + n_{d,3}, \text{ where } \mathbf{x} = \sqrt{P_r} \frac{\mathbf{h}_{rd, l^*}^H}{\|\mathbf{h}_{rd, l^*}\|}, \quad (36)$$

and the $S \rightarrow R_{l^*} \rightarrow D$ SNR is equal to:

$$\rho_{srd, l^*}^{(RHtT)} = \frac{1}{\sigma^2} \frac{G_{sr, l^*} P_s P_r \|\mathbf{h}_{rd, l^*}\|^2}{G_{sr, l^*} P_s + P_r \|\mathbf{h}_{rd, l^*}\|^2 + \sigma^2}. \quad (37)$$

In what follows, we discuss the rate optimal system design for RHtT.

2) *Optimizing the RHtT Scheme:* Using (7) and the above analysis, the joint energy causality and energy preservation constraints for RHtT are expressed as:

$$P_r \leq \frac{2e_{s, l^*}^{(RHtT)} (\mathbf{f}_2^H \hat{\mathbf{H}} \mathbf{f}_2)}{(1 - \theta) T} - \varepsilon P_C^{(RHtT)} = P_r^{(RHtT)} (\mathbf{f}_2^H \hat{\mathbf{H}} \mathbf{f}_2), \quad (38)$$

where $e_{s, l^*}^{(RHtT)} (\mathbf{f}_2^H \hat{\mathbf{H}} \mathbf{f}_2)$ the energy surplus for RHtT⁵. It is then easy to see the RHtT rate optimization problem has a similar structure as the one of (P3), with the difference being that parameters a and β are not involved, since the beamformer at R_l^* is predetermined. Therefore, we can finally suboptimally solve problem (P3) by modifying Algorithm 2 such as to exclude Step 5 (since no calculation of a beamformer at the relay is required) and substituting the SNR in Step 6 by the definition in (37), with P_r selected such that (38) is satisfied with equality.

IV. FINALIZING OUR SYSTEM MODEL

In the following two subsections we treat the remaining details of our system model.

A. Determining Parameters θ and m_{l^*} and acquiring Channel State Information (CSI)

As we have seen in [14], for a single-antenna S , nearly optimal values for θ can be found by using Golden Section Search (GSS). Motivated by this, we propose using GSS and set (as in [14]) the number of GSS iterations for selecting θ , as low as 10. Moreover, we apply this process for all candidate m_{l^*} values in order to select the optimal EH antenna. Finally, the CSI for optimizing our schemes, can be obtained using the methodology of [14]. This includes using a Channel Estimation (CE) subframe at every TF and performing $S \rightarrow R_l$ CE at R_l and $R_l \rightarrow D$ channel estimation at D . The power consumption that needs to be spent in order to perform CE at R_l , can then be included in P_C [14]. Further mechanisms for CSI acquisition are found in [14] along with methods for accounting for the power consumption of CE.

⁵From (6), this is equal to $e_{s, l^*}^{(RHtT)} = E_{l^*}^{(start)} + e_{h, l^*, 1} + e_{h, l^*, 2} (\mathbf{f}_2^H \hat{\mathbf{H}} \mathbf{f}_2) - E_{l^*}^{(0)}$.

B. Relay Selection and Operation at the Non Selected Relays

Aiming at optimizing the instantaneous rate, we consider solving the optimal system design problem (i.e., determination of θ and m_{l^*} , and design of beamformers) for all relays, and then selecting as R_{l^*} the relay that results in the maximum instantaneous transmit rate. Having determined R_{l^*} , relays $R_l, l \neq l^*$, apply EH for the whole TF, employing antenna m_l , and the signals reaching antenna m_l of R_l during phases I and II are expressed as:

$$\begin{aligned} y_{r,l,1} &= \mathbf{h}_{sr,l} \mathbf{f}_1 \sqrt{P_s} x_e + n_{r,l,1}, \text{ and} \\ y_{r,l,2} &= \mathbf{h}_{sr,l} \mathbf{f}_2 \sqrt{P_s} x_d + n_{r,l,2}, \end{aligned} \quad (39)$$

where $\mathbf{h}_{sr,l} = \mathbf{H}_{sr,l}(m_l, :)$, and $n_{r,l,1}, n_{r,l,2}$, the noise during phase I and II at antenna m_l respectively. Finally, the signal reaching antenna m_l during phase III, is written as:

$$y_{r,l,3} = \mathbf{h}_{sr,l} \mathbf{f}_3 x_d e^{j\psi} + \frac{\mathbf{h}_{l^*,l} \mathbf{x} y_{r,l^*,2}^{(d)}}{\sqrt{G_{sr,l^*} + \sigma^2}} + n_{d,3}, \quad (40)$$

where $\mathbf{h}_{l^*,l}$ the channel formed between the transmit antennas of R_{l^*} and the EH antenna of l . Clearly, (40) is a generic equation which applies to both RHtTH and RHtT. This means that its exact form varies for the two schemes according to the dimensions of vectors \mathbf{x} and $\mathbf{h}_{l^*,l}$ for each scheme. The total harvested energy during a TF by R_l is then equal to:

$$\begin{aligned} E_{h,l} &= \theta T P_h (|\mathbf{h}_{sr,l} \mathbf{f}_1|^2) + \frac{(1-\theta) T P_h (|\mathbf{h}_{sr,l} \mathbf{f}_2|^2)}{2} \\ &+ \frac{(1-\theta) T P_h \left(|\mathbf{h}_{sr,l} \mathbf{f}_3 e^{j\psi} + \mathbf{h}_{l^*,l} \mathbf{x} \sqrt{\frac{\rho_{sr,l^*}}{\rho_{sr,l^*} + 1}}|^2 \right)}{2}, \end{aligned} \quad (41)$$

where ρ_{sr,l^*} is the SNR on the $S \rightarrow R_{l^*}$, for the considered scheme (i.e., RHtTH or RHtT). This amount of energy is added to the energy available at the battery of R_l , at the beginning of the TF, such as to determine the energy available to R_l at the beginning of the following TF. Clearly, $E_{h,l}$ is a function of m_l . However, since performing antenna selection such as to maximize the harvested energy at non-selected relays requires channel information for $\mathbf{h}_{l^*,l}$ that can be difficult to obtain, we assume that for non-selected relays, a fixed antenna (e.g., the first one) is always selected for EH. With this assumption $\mathbf{h}_{sr,l}$ is equal to $\mathbf{h}_{sr,l} = \mathbf{H}_{sr,l}(1, :)$.

C. Practical Considerations

In this subsection, several practical considerations related to our schemes are discussed.

1) *Optimizing systems using M-ary QAM*: In case of systems that employ practical modulation schemes (e.g., M-ary Quadrature Amplitude Modulation (QAM)), Shannon capacity might not serve as a representative rate metric. However, our methods can also optimize the rate of such systems. In more detail, introducing again the energy causality and energy preservation constraints along with the constraint that the M-QAM Bit Error Rate (BER), hereby denoted as $P_e(\rho, M)$ with ρ being the SNR, is below a predetermined target value $P_e^{(t)}$,

and a TF duration T , being integer multiple of T_s , the rate optimal design problem for RHtTH is expressed as:

$$\begin{aligned} \text{maximize}_{\mathbf{f}_2, \mathbf{x}, \theta} &: \frac{(T - \theta T) \log_2 M}{2T}, \\ \text{s.t.} &: \|\mathbf{f}_2\|^2 = 1, \quad (16), \quad P_e(\rho^{(RHtTH)}, M) \leq P_e^{(t)}, \\ &\text{and } \theta T = k T_s, k \in \left\{ 0, 1, \dots, \frac{T}{T_s} \right\}. \end{aligned} \quad (P9)$$

It is then easy to show that (P9) can be solved by starting with $k = 0$ and progressively increasing its value. For each new candidate value of k , the corresponding SNR-optimal beamformers need to be found. This can be done by using our Section III methods. Provided that the obtained beamformers satisfy the constraints of (P9), the optimal value of k is obtained. Otherwise, higher values of k should be considered. A similar approach can be followed also for the case of RHtT.

2) *Complexity and CSI considerations*: As the number of relays increases, the CSI that has to be collected in order to apply the relay selection policy also increases. As a result, assuming that the optimal system design problem is solved at S , a significant communication/signaling overhead is added, because all relays should forward the collected CSI to S . Moreover, the complexity of solving the optimal system design problem for all relays also becomes significant.

3) *Robustness to channel estimation errors*: In various communication scenarios, non-negligible channel estimation errors exist. For these cases, the system design should be revised, such as to account for the uncertainty that the imperfect CSI introduces in the calculation of the energy that can be harvested. Alternatives, schemes exploiting statistical CSI could be considered [28].

4) *Hardware constraints*: A further constraint for WPRNs is the limited sensitivity of the EH circuit, which results in harvesting no power when the input power is low. However, the generic nature of our EHM model allows to optimize systems which suffer from this constraint.

5) *Operation in the presence of interference*: In case of coexistence of multiple WPRNs, the effect of interference needs to be taken into account and/or exploited. In more detail, assuming multiple WPRNs with multiple sources, coordination, and synchronization among the them may assist towards ensuring higher amounts of harvested energy at the relays. However, the signal transmissions of the multiple sources during phases II and III should take into account the impact of interference in signal reception at the relays.

V. NUMERICAL RESULTS

To assess our schemes, we performed extensive simulations using the parameters of Table III for single- and two-relay scenarios. The following summarizes our findings.

A. Single Relay Scenario in the presence of EH non-linearities

We consider a single relay scenario and place S at coordinates $(0, 0)$, D at coordinates $(d_{sd}, 0)$, and R at coordinates of the form $(x_r, d_{sd}/10)$, where d_{sd} the $S \rightarrow D$ distance, selected to be equal to 30 meters (as in [14]). Employing the parameters used in [14], we calculate the pathloss at a distance

TABLE III: Simulation parameters of the proposed system

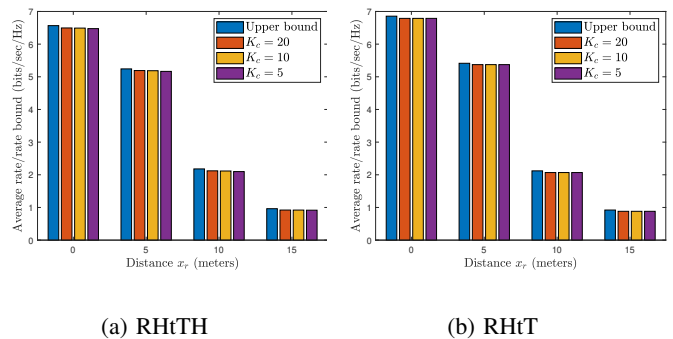
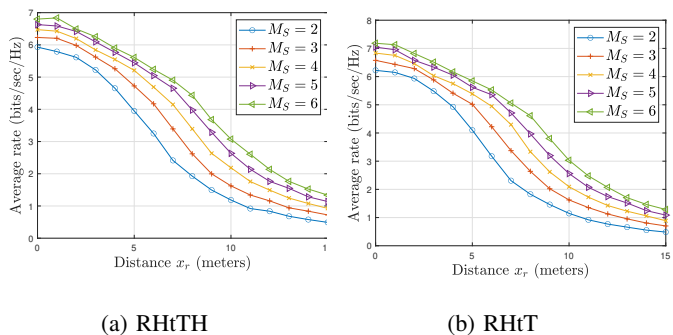
Parameter	Value
Carrier frequency	915MHz
(M_S, M_R)	(4,3)
Pathloss exponent	2.5
ε	0.75
d_{sd}	30 meters
(P_c, P_{tx}, P_{rx}) (in $\mu Watts$)	(50, 20, 20)
\mathcal{G}_t	10[dB]
T	1 second
K factor on the $S \rightarrow R_l$ Rice fading channel	5[dB]
\mathbf{h}_{loop}	$\sqrt{10^{-1.2}} \mathbf{1}_{M \times 1}$
(P_s, σ^2) (in dBm)	(30, -90)

d from a transmitter as $PL(d) = \frac{\mathcal{A}\mathcal{G}_t}{(d/d_0)^p}$, where $d_0 = 1$ meter is a reference distance, $\mathcal{A} = 0.001$ the pathloss at this distance, $p = 2.5$ the pathloss exponent and \mathcal{G}_t the transmit antennas gain. In addition to pathloss, we assume Line-of-Sight (LoS) conditions modeled as independent and identically distributed (i.i.d.) narrowband Rice fading on the $S \rightarrow R$ channel and set the K -factor to 5dB. On the other hand, we model the $R \rightarrow D$ channel as an i.i.d. narrowband Rayleigh fading channel. To model EH, We use a non-linear EHM where the harvested power (in Watts) from an input signal of average power P_{in} (in Watts) is given as [9], [29]:

$$P_{out} = P_h(P_{in}) = \frac{\Psi - M_H \Theta}{1 - \Theta}, \quad (43)$$

where $\Theta = \frac{1}{1 + \exp(a_H b_H)}$ and $\Psi = \frac{M_H}{1 + \exp(-a_H(P_{in} - b_H))}$, where parameters M_H, a_H, b_H allow to fit the EHM to EH circuit measurements. For the selected carrier frequency, we set $(M_H, a_H, b_H) = (0.024, 150, 0.014)$ as in [29]. Note that EHMs of the form (43) are among the most popular EHMs in the literature and satisfy our assumption of being non-decreasing. The power levels at S for RHtTH and RHtT were selected such that the energy transmitted by S for every TF, during which a transmission takes place, is equal to 1Joule. Assuming a TF duration of $T = 1$ second, the power level for RHtTH was therefore equal to $P_s = 30dBm$, while for RHtT, given that in RHtT S is silent during phase III, the transmit power was equal to $\hat{P}_s = \frac{2P_s}{1+\theta}$. Moreover, for any channel realization, if for some scheme the rate optimal system design problem was found to be infeasible, the instantaneous rate of the particular scheme was set equal to zero and both the source and the relay would remain idle.

In Fig. 1a we present the average RHtTH rate for different values of x_r , for $K_\gamma = 5$ and different K_c values. In the same plot we show the average rate upper bounds obtained by averaging the bounds derived in Appendix C, for each channel realization. Fig. 1a reveals that K_c values as low as $K_c = 5$, result in performance which is less than 5% smaller than the upper bound, for all x_r values. As a result, even for small K_c values, suboptimal BF combined with GSS for determining θ , results in near optimal performance. Similarly, selecting K_γ as low as $K_\gamma = 5$, results in near-optimal performance. Furthermore, in Fig. 1b we present the average rate for the same values of x_r , for RHtT for different choices of K_c . The results confirm again that low K_c values, combined with GSS, achieve near-optimal performance.

Fig. 1: The average rates and their upper bounds vs x_r , for various K_c values and a single relay.Fig. 2: The average rate as a function of x_r , for a single relay, and different values of M_S .

1) *Performance as a function of M_S* : In Fig. 2a we plot the performance of RHtTH for $K_c = 5$ and $K_\gamma = 5$ for different M_S values. The remaining parameters are given in Table III. We observe that although the increase of M_S from 2 to 3 results in significant performance benefits, further increase of M_S results in progressively reduced additional performance benefits. Furthermore, in Fig. 2b, we present the performance of RHtT as a function of x_r , for different values of M_S , reaching the same conclusion.

2) *Performance as a function of M_R* : To investigate the performance as a function of M_R , we set $M_S = 4$ and consider $M_R \in \{3, 4, 5, 6\}$. The results for RHtTH and RHtT are shown in Figs. 3a and 3b respectively, and show that for large values of x_r , increasing M_R results in lower average transmission rate. In particular, for both schemes, for $x_r > 7$ meters, selecting $M_R = 3$ results in better average rate than the choice $M_R = 6$. This is explained by the fact that the power consumption of the relay increases as M_R increases. Therefore, for larger $S \rightarrow R$ distances, the fact that lower values of M_R result in smaller power consumption, results in transmitting more often and with higher power at R . The achievable average rate is therefore increased.

3) *Studying the impact of power consumption and the WPT phase and comparing to benchmarks*: In Fig. 4a, we investigate the impact of the WPT phase on the performance. To this end, we consider the case that the WPT phase is omitted (i.e., we set $\theta = 0$ for all TFs) and compare it with

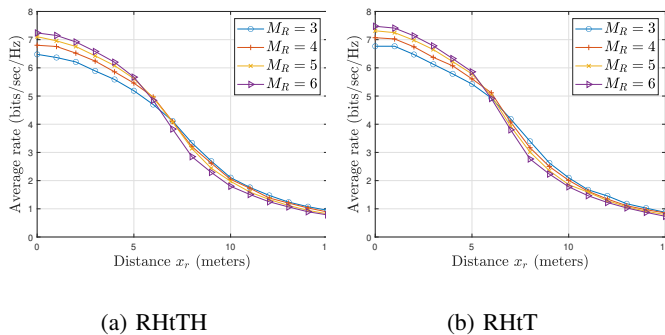
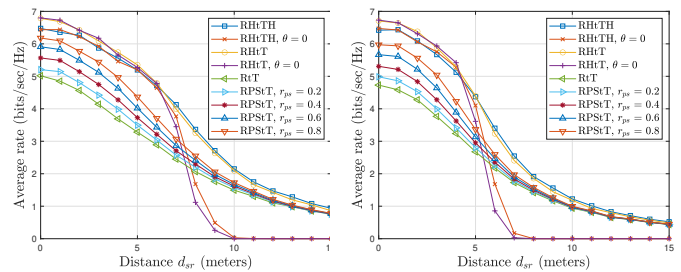


Fig. 3: The average rate as a function of x_r , for a single relay, and different values of M_R .

the case that GSS is applied on each TF in order to determine θ . In the same figure, for benchmarking purposes, we also present the performance of two schemes that are based on traditional WPR techniques i.e., PS and/or TS. We refer to these schemes as RtT (i.e., Receive then Transmit) and as RPStT (i.e., Receive and Power Split then Transmit). RtT is obtained if, following the WPT subframe, all antennas at R are used for data reception during phase II and data forwarding during phase III. RPStT is obtained if during Phase II, one of the relay antennas uses a power splitter in order to combine data reception with EH. Further information about these two benchmarks are given in Appendix D. RtT is a fair benchmark, because no other scheme in the literature exploits exactly the same hardware as RHtTH and RHtT and just like RHtTH and RHtT is EHM agnostic. On the other hand, RPStT assumes the existence of a power splitter at the relay, used in order to harvest a portion of the energy received by an antenna of the relay during phase II. The power splitting coefficient, i.e., the portion of power that is going to be used for EH purposes (denoted as r_{ps} in Appendix D), is selected to be constant, and different values (from the set $\{0.2, 0.4, 0.6, 0.8\}$) are considered for it. Clearly, RPStT is indicative of the performance that can be achieved by combining two classical WPT techniques, i.e., TS and PS. From the results shown in Fig. 4a, we obtain that for $x_r \leq 6$ meters, the performance of RHtT remains the same even if the WPT phase is omitted. The same also holds for RHtTH. For higher values of x_r , for both schemes, the presence of the WPT phase delivers important performance benefits. This is explained by the fact that for small values of x_r , the relay is able to harvest sufficient amounts of energy, even if the WPT phase is omitted. However, as x_r increases, the contribution of the WPT phase to EH is elevated. A further advantage of the presence of the WPT phase is that it reduces the time spent on transmitting and/or receiving and may allow for transmissions of smaller duration but with higher transmission power. As a result, introducing a WPT phase results in better energy management, and reduces the percentage of power that is consumed by the relay's circuits. This is important when the $S \rightarrow R$ distance increases and EH cannot deliver large amounts of energy. Finally, both RHtTH and RHtT outperform RtT and RPStT, for all values of the power splitting factor.



(a) Power consumption parameters of Table III. (b) Power consumption parameters (doubled) of Table III.

Fig. 4: The average rate as a function of x_r in the presence and absence of the WPT phase, for two power consumption parameters and a single relay scenario.

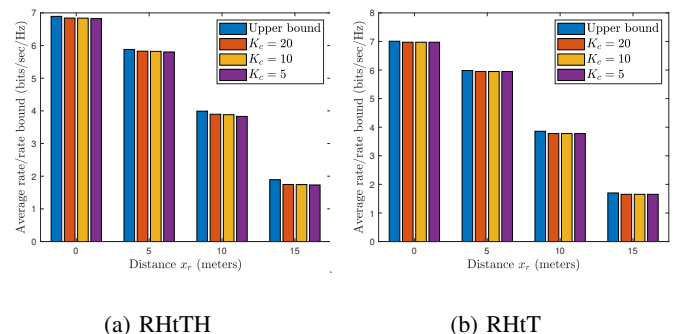


Fig. 5: The average rate and its bound versus x_r , for the linear EHM, for different K_c values.

We now repeat our simulations after doubling the P_{tx} , P_{rx} , and P_{circ} values presented in Table III. The resulting average rates are given in Fig. 4b and show that the WPT phase becomes more significant, delivering substantial performance gains for $x_r > 4$ meters. As a result, comparing Figs. 4a and 4b, we see that performance gains delivered by the WPT phase are more significant in case of high power consumption. Again, both our schemes outperform RtT and RPStT.

B. Single relay scenario with a linear EHM

We also assessed our schemes for an EHM, where the input-output power relation for the EH circuit is given as $P_h = \eta P_{in}$, with $\eta = 0.75$. In Figs. 5a and 5b, we compare the performance achieved by RHtT and RHtTH for different K_c values, with the average rate upper bounds obtained by the process in Appendix C, for this EHM. The results confirm that our low complexity solutions combined with a small number of GSS iterations, deliver again near optimal performance. Hence, for the remaining of the paper we will only consider the non-linear EHM, which is more realistic. Also, having confirmed the proximity of the achievable rate with its upper bound, in what follows we will be only presenting the results obtained by our algorithms.

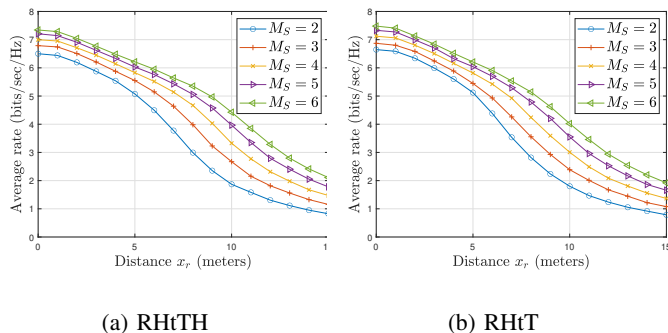


Fig. 6: The average RHtTH and RHtT rates vs x_r , for 2 relays and various M_S values.

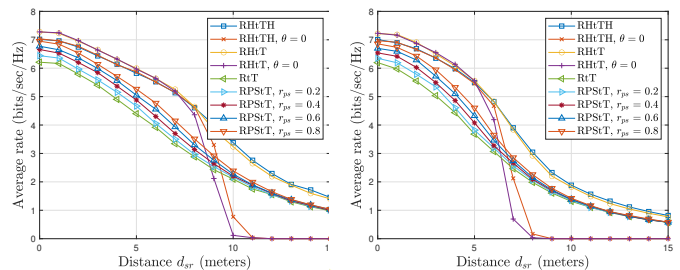
C. Two Relays Scenario in the presence of EH non-linearities

In order to study the impact of multiple relays, we focus on a communication scenario, where two relays are available for communication and EH purposes. Such a scenario is close to practical communication situations (where even if a larger number of relays is available, probably only a small subset of them will be dedicated to facilitating a particular destination). This is the reason why this scenario has been also adopted by many researchers in the past and even system designs tailored to this scenario have been introduced, e.g., [30], [31]. We place the two relays at coordinates of the form $(x_r, \pm \frac{d_{sd}}{10})$, and study the performance of all schemes. Assuming i.i.d. Rice fading on the $S \rightarrow R_l$ links and Rayleigh fading on the $R_l \rightarrow D$ links, $l = 1, 2$, we study the performance for the parameter values in Table III. In what follows we summarize our results.

1) *Performance as a function of M_S* : In Fig. 6a and Fig. 6b, we present the performance of RHtTH and RHtT respectively, as a function of x_r , for different values of M_S . From both figures, we see that increasing M_S , results in improved performance and that the performance benefits delivered by increasing M_S by one, are high only for small values of M_S .

2) *Performance as a function of M_R* : Using the simulation parameters of Table III for a system with two relays, the same qualitative results were observed. This means, that as in the single-relay case, for $x_r \geq 6$ meters, high values of M_R resulted in lower rate than low values of M_R . This is due to the fact that increasing M_R also increases the power consumption.

3) *Studying the impact of the power consumption and the WPT phase and comparing with benchmarks*: Fig. 7a presents the performance of our schemes and of RtT (with rate optimal relay selection) for the parameters of Table III. Comparing Fig. 7a with Fig. 4a, we see that adding a second relay increases the range of x_r values for which omitting the WPT phase does not result in a performance degradation. In Fig. 7b we repeat our simulations, after doubling the power consumption parameter values. By comparing Fig. 7b with Fig. 4b we reach the same conclusion, with the only difference being that the point after which the use of the WPT phase results in notable performance differences is shifted to the right (w.r.t. the single



(a) Power consumption parameter- (b) Performance after doubling the power consumption.

Fig. 7: The average rate as a function of the power consumption parameters, for 2 relays.

relay case). Superiority of RHtTH and RHtT (w.r.t. RtT and RPSiT) is again confirmed.

VI. SUMMARY AND CONCLUSIONS

We studied multi-antenna (at S and R) WPRNs, and proposed, optimized, and compared two different communication schemes. In what follows, we summarize our findings:

1) *Near optimal performance can be combined with low complexity*: Section V results demonstrate that for both schemes, for relays placement close to S , near-optimal performance is achieved even if the WPT phase is omitted. The complexity of selecting θ is then avoided.

2) *Low complexity BF delivers near optimal performance*: The results of Section V illustrate that our low complexity RHtTH and RHtT BF techniques deliver average rate values very close to the optimal ones.

3) *The optimal scheme varies as a function of the distance between S and the relays*: Section V results show that, for small $S \rightarrow R_l^*$ distances, RHtT is the optimal scheme. However, for large $S \rightarrow R_l^*$ distances, RHtTH outperforms RHtT. Hence, as the distance between S and the relays increases, the complexity for delivering near optimal performance increases, due to the increasing importance of the WPT, and the fact that RHtTH results in increased complexity (w.r.t. RHtT), since it requires solving the BF problem at the relays.

4) *GSS delivers near optimal performance*: Figs. 1a, 1b, 5a, 5b confirm that a small number of iterations of GSS results in near optimal performance.

Finally, we verified that our proposed schemes outperform existing benchmarks.

APPENDIX A SOLVING (P4) AND (P1)

By introducing the matrix $\mathbf{F} = \mathbf{f}_2 \mathbf{f}_2^H$ and working as in [32], problem (P4) is rewritten as:

$$\begin{aligned} \underset{\mathbf{F}}{\text{maximize}}: & \text{tr}(\hat{\mathbf{H}}\mathbf{F}) \quad \text{s.t.:} \quad \text{tr}(\tilde{\mathbf{H}}\mathbf{F}) = c, \text{tr}(\mathbf{F}) = 1, \\ & \text{rank}(\mathbf{F}) = 1, \mathbf{F} \succeq 0. \end{aligned} \quad (\text{P2.1})$$

By dropping the constraint $\text{rank}(\mathbf{F}) = 1$, the Semidefinite Programming (SDP) relaxation of (P2.1) is obtained, which

can be solved with complexity $\mathcal{O}\left((2M_S)^{4.5} \log(1/\epsilon)\right)$, where ϵ an accuracy parameter [32]. Moreover, it is known that for a complex valued SDP with q constraints, an optimal solution \mathbf{F}^* can be found, for which $\text{rank}(\mathbf{F}^*) \leq \sqrt{q}$, [32]. Applying this property to the SDP relaxation of (P2.1), yields that rank-one solutions \mathbf{F}^* can be obtained, which are also solutions to (P2.1)⁶. Optimal \mathbf{f}_2 is then the eigenvector corresponding to $\lambda_{max}(\mathbf{F}^*)$.

APPENDIX B

SOLVING PROBLEMS OF THE FORM (P8) AND (P8.1)

Problems (P8) and (P8.1) are instances of the problem:

$$\begin{aligned} & \text{maximize: } \alpha\gamma_1 + \beta\gamma_2, \text{ s.t.: } \gamma_1^2 + \gamma_2^2 \leq P, \gamma_1 \in [\gamma_{low}, \gamma_{up}], \\ & \gamma_1 \in \mathbb{R}^+, \gamma_2 \in \mathbb{R}^+ \end{aligned} \quad (45)$$

for some γ_{low} and γ_{up} , and the the optimal γ_2 is given as $\gamma_2^* = \sqrt{P - \gamma_1^{*2}}$ [12], while the optimal γ_1 , i.e., γ_1^* , is equal to $\gamma_1^{(cand)} = \sqrt{\alpha^2 P / (\alpha^2 + \beta^2)}$, provided that $\gamma_1^{(cand)} \in [\gamma_{low}, \tilde{\gamma}_{up} = \min\{\sqrt{P}, \gamma_{up}\}]$. Otherwise, γ_1^* is the value from the set $\{\gamma_{low}, \tilde{\gamma}_{up}\}$ resulting in the highest value for the UF. Finally, parameters α, β , and P remain the same regardless of K_γ . Hence, for each channel realization, $\gamma_1^{(cand)}$ needs to be calculated once. Therefore, the worst case complexity of (P8) and (P8.1) can be found to be equal to 7 multiplications, 4 additions and 2 square root calculations.

APPENDIX C

BOUNDING THE TRANSMIT RATE

Let $\theta \in [\underline{\theta}, \bar{\theta}]$ for $\underline{\theta} \in [0, \bar{\theta})$, and $\bar{\theta} \in (0, 1)$. Exploiting upper bounds $e_{up,l^*,i}$ for $e_{h,l^*,i}$, $i = 1, 2, 3$, relaxed versions of the energy preservation and energy causality constraints can be constructed. Assuming that R_{l^*} uses a beamformer \mathbf{x} with $\|\mathbf{x}\|^2 = P_r$, it is then easy to show that an upper bound $\bar{\rho}_{srd,l^*}(\underline{\theta}, \bar{\theta})$ for the $S \rightarrow R_{l^*} \rightarrow D$ SNR is found by solving the problem:

$$\begin{aligned} & \text{maximize: } \rho_{srd,l^*} \text{ s.t.: } \|\mathbf{f}_2\|^2 = 1, \text{ and} \\ & \mathbf{f}_2, \mathbf{x} \\ & \|\mathbf{x}\|^2 \leq \frac{2\epsilon e_{s,up,l^*}}{(1-\bar{\theta})T} + \frac{2\epsilon \min\{e_{up,l^*,3}, E_{l^*}^{(0)}\}}{(1-\bar{\theta})T} - \epsilon P_C. \end{aligned} \quad (46)$$

The maximum rate is then bounded by the quantity: $R_{up}(\underline{\theta}, \bar{\theta}) = \frac{(1-\underline{\theta})T}{2} \log_2(1 + \bar{\rho}_{srd,l^*}(\underline{\theta}, \bar{\theta}))$. We further explain this approach for RHtTH and RHtT.

A. Bounding the RHtTH SNR and Rate for $\theta \in [\underline{\theta}, \bar{\theta}]$

Exploiting the optimal structure of \mathbf{x} , the following upper bounds for $e_{h,l,i}$ are found:

$$\begin{aligned} e_{up,l^*,1} &= \bar{\theta} T P_h(\max\{\mathbf{H}_{sr,l}(m, :)\}), \\ e_{up,l^*,2} &= e_{up,l^*,2}^{(RHtTH)}(\mathbf{f}_2^H \hat{\mathbf{H}} \mathbf{f}_2) = \frac{(1-\underline{\theta})T}{2} P_h(\mathbf{f}_2^H \hat{\mathbf{H}} \mathbf{f}_2 P_s), \\ e_{up,l^*,3}^* &(\mathbf{f}_2^H \hat{\mathbf{H}} \mathbf{f}_2, \gamma_1) = \frac{(1-\underline{\theta})T}{2} P_h(P_{in,l^*,3}^{(opt)}(\mathbf{f}_2^H \hat{\mathbf{H}} \mathbf{f}_2, \gamma_1)). \end{aligned} \quad (47)$$

⁶If the solution obtained by solving the relaxed SDP is not rank-one, a rank-one solution for it can still be constructed following the process proposed in [33].

Moreover, from (P3), the $S \rightarrow R_{l^*} \rightarrow D$ SNR is equal to $\rho_{srd,l^*}^{(RHtTH)} = \frac{1}{\sigma^2} \frac{\mathbf{f}_2^H \hat{\mathbf{H}} \mathbf{f}_2 P_s (\alpha\gamma_1 + \beta\gamma_2)^2}{\mathbf{f}_2^H \hat{\mathbf{H}} \mathbf{f}_2 P_s + (\alpha\gamma_1 + \beta\gamma_2)^2}$. Using (47) and ρ_{srd,l^*} , we proceed to calculate an upper bound on the optimal UF value of (46). To do so, we add the constraint $\underline{c} \leq \mathbf{f}_2^H \hat{\mathbf{H}} \mathbf{f}_2 \leq \bar{c}$ to (46). Given this constraint, working as in Appendix A, $\mathbf{f}_2^H \hat{\mathbf{H}} \mathbf{f}_2$ is upper bounded by the UF value at the solution of the problem:

$$\begin{aligned} & \text{maximize: } \text{tr}(\hat{\mathbf{H}} \mathbf{F}) \text{ s.t.: } \underline{c} \leq \text{tr}(\tilde{\mathbf{H}} \mathbf{F}) \leq \bar{c}, \text{tr}(\mathbf{F}) = 1, \mathbf{F} \succeq 0, \\ & \mathbf{F} \end{aligned} \quad (48)$$

which can be solved using CVX. Let $Q_{up}(\underline{c}, \bar{c})$ be the optimal UF value of (48). By setting $\mathbf{f}_2^H \hat{\mathbf{H}} \mathbf{f}_2 = Q_{up}(\underline{c}, \bar{c})$, an upper bound to $\rho_{srd,l^*}^{(RHtTH)}$ is obtained if γ_1, γ_2 are solutions to the problem:

$$\begin{aligned} & \text{maximize: } \alpha\gamma_1 + \beta\gamma_2 \\ & \gamma_1 \in \mathbb{R}^+, \gamma_2 \in \mathbb{R}^+ \end{aligned} \quad (P10)$$

$$\text{s.t.: } \gamma_1^2 + \gamma_2^2 \leq$$

$$\begin{aligned} & \frac{2\epsilon \left(E_{l^*}^{(start)} + e_{up,l^*,1} + e_{up,l^*,2}^*(\underline{c}, \bar{c}) + \min\left\{0, \left(e - E_{l^*}^{(0)}\right)\right\} \right)}{(1-\bar{\theta})T} \\ & - \epsilon P_C^{(RHtTH)} \end{aligned} \quad (C10.1)$$

with $e_{up,l^*,2}^*(\underline{c}, \bar{c}) = e_{up,l^*,2}^{(RHtTH)}(Q_{up}(\underline{c}, \bar{c}))$. We now bound the optimal UF value of (P10).

1) *Bounding the optimal UF value of (P10)*: We first bound the feasible values of γ_1 in (P10). To do so, we assume a sequence $\gamma_{max}^{(0)}, \dots, \gamma_{max}^{(n-1)}$, of descending upper bounds for the maximum feasible value of γ_1 in (C10.1). Using $\gamma_{max}^{(n-1)}$ and setting $\gamma_2 = 0$ in (C10.1), we then obtain as a new candidate upper bound for γ_1 the value:

$$\gamma_{new}^2 = P_{up}^{(RHtTH)}(\underline{c}, \bar{c}, e_{up,l^*,3}^*(\bar{c}, \gamma_{max}^{(n-1)})). \quad (50)$$

If $\gamma_{new} < \gamma_{max}^{(n-1)}$ we can then set $\gamma_{max}^{(n)} = \gamma_{new}$. This process can be repeated, after substituting $\gamma_{max}^{(n-1)}$ by $\gamma_{max}^{(n)}$ in (49), in order to obtain further, stricter bounds. To apply this process, a starting bound $\gamma_{max}^{(0)}$ is needed. To find it, we set $\gamma_2 = 0$ in (C10.1). Since $\min\left\{0, \left(e_{up,l^*,3}^*(\bar{c}, \gamma_{max}^{(n-1)}) - E_{l^*}^{(0)}\right)\right\} \leq 0$, the following starting upper is then found:

$$\gamma_{max}^{(0)} = \sqrt{P_{up}^{(RHtTH)}(\underline{c}, \bar{c}, E_{l^*}^{(0)})}. \quad (51)$$

Exploiting $\gamma_{max}^{(n)}$: Taking advantage of $\gamma_{max}^{(n)}$, we can bound the UF value at the solution of (P10) by adding the constraint $\gamma \in [\underline{\gamma}, \bar{\gamma}] \subset [0, \gamma_{max}^{(n)})$ to (P10) and forming the problem:

$$\begin{aligned} & \text{maximize: } (\alpha\gamma_1 + \beta\gamma_2), \text{ s.t.: (C10.1), } \gamma_1 \in [\underline{\gamma}, \bar{\gamma}]. \\ & \gamma_1 \in \mathbb{R}^+, \gamma_2 \in \mathbb{R}^+ \end{aligned} \quad (P11.1)$$

Due to the non-decreasing form of $P_h(\cdot)$, it is straightforward to upper bound the value of the UF of (P11.1) by substituting $e_{up,l^*,3}^*(\bar{c}, \gamma_1)$ by $e_{up,l^*,3}^*(\bar{c}, \bar{\gamma})$ and considering the problem:

$$\begin{aligned} & \text{maximize: } (\alpha\gamma_1 + \beta\gamma_2) \text{ s.t.: } \gamma_1 \in [\underline{\gamma}, \bar{\gamma}], \\ & \gamma_1 \in \mathbb{R}^+, \gamma_2 \in \mathbb{R}^+ \\ & \gamma_1^2 + \gamma_2^2 \leq P_{up}^{(RHtTH)}(\underline{c}, \bar{c}, e_{up,l^*,3}^*(\bar{c}, \bar{\gamma})) = P_r^{(up)}, \end{aligned} \quad (P12)$$

which is solved using the process in Appendix B. Let γ_1^* be the obtained solution. By defining:

$$U(\underline{\gamma}, \bar{\gamma}; \underline{c}, \bar{c}, \underline{\theta}, \bar{\theta}) = \alpha \gamma_1^* + \beta \sqrt{P_r^{(up)} - \gamma_1^{*2}}, \quad (53)$$

and using a set of points $\gamma_{1,0} = 0 < \gamma_{1,1} < \dots < \gamma_{1,N+1} = \gamma_{max}^{(n)}$, we can then upper bound the optimal UF value in (P11.1), by the quantity $U(\underline{c}, \bar{c}; \underline{\theta}, \bar{\theta}) = \max \{U(\gamma_{1,i}, \gamma_{1,i+1}; \underline{c}, \bar{c}, \underline{\theta}, \bar{\theta})\}_{0 \leq i \leq N}$.

Hence, for $c \in [\underline{c}, \bar{c}]$, we can bound $\rho_{srd,l^*}^{(RHtTH)}$ by: $\bar{\rho}_{srd,l^*}^{(RHtTH)}(\underline{\theta}, \bar{\theta}; \underline{c}, \bar{c}) = \frac{1}{\sigma^2} \frac{\bar{c} P_s U^2(\underline{c}, \bar{c}; \underline{\theta}, \bar{\theta})}{\bar{c} P_s + U^2(\underline{c}, \bar{c}; \underline{\theta}, \bar{\theta}) + \sigma^2}$. Building on this upper bound and using a set of points $c_{min} = c_0 < c_1 < c_2 < \dots < c_N < c_{N+1} = c_{max}$, we can then obtain the following upper bound for the $S \rightarrow R_l^* \rightarrow D$ rate:

$$\begin{aligned} \bar{R}_{up}(\underline{\theta}, \bar{\theta}) &= \frac{(1-\underline{\theta})T}{2} \\ &= \log_2 \left(1 + \max \left\{ \bar{\rho}_{srd,l^*}^{(RHtTH)}(\underline{\theta}, \bar{\theta}; c_i, c_{i+1}) \right\}_{0 \leq i \leq N} \right). \end{aligned} \quad (54)$$

B. Bounding the RHtT SNR and Rate for $\theta \in [\underline{\theta}, \bar{\theta}]$

Using $e_{up,l^*,1}$ in (47), the fact that $e_{h,l^*,2}$ is upper bounded by $e_{up,l^*,2}^{(RHtTH)}$ and working as for RHtTH, for $c \in [\underline{c}, \bar{c}]$, the optimal SNR value is upper bounded by:

$$\bar{\rho}_{srd,l^*}^{(RHtT)}(\underline{\theta}, \bar{\theta}; \underline{c}, \bar{c}) = \frac{1}{\sigma^2} \frac{\bar{c} P_s \|\mathbf{h}_{rd,l^*}\|^2 P_{up}(Q_{up}(\underline{c}, \bar{c}))}{\bar{c} P_s + \|\mathbf{h}_{rd,l^*}\|^2 P_{up}(Q_{up}(\underline{c}, \bar{c})) + \sigma^2}. \quad (55)$$

Therefore, using points $c_{min} = c_0 < \dots < c_{N+1} = c_{max}$, we find the following rate bound:

$$\begin{aligned} R_{up}(\underline{\theta}, \bar{\theta}) &= \frac{(1-\underline{\theta})T}{2} \\ &\times \log_2 \left(1 + \max \left\{ \bar{\rho}_{srd,l^*}^{(RHtT)}(\underline{\theta}, \bar{\theta}; c_i, c_{i+1}) \right\}_{1 \leq i \leq N} \right). \end{aligned} \quad (56)$$

C. Constructing a Final Bound on the Achievable Rate

Using a set of points $0 = \theta_0 < \dots < \theta_{N+1} = 1$, we can finally upper bound the achievable rate for each scheme by the quantity $R_{up} = \max \{R_{up}(\theta_i, \theta_{i+1})\}_{0 \leq i \leq N}$. Repeating this process for any candidate m_{l^*} this upper bound is generalized in case that EH antenna selection is applied.

APPENDIX D

PERFORMANCE BENCHMARKS FOR THE CONSIDERED SCHEMES

We start by presenting RPSSt. Following that, we treat RtT as a special case of RPSSt.

⁷For $\theta \in [\theta_N, 1]$, since the $S \rightarrow R_l^*$ rate is an upper bound on the $S \rightarrow R_l^* \rightarrow D$ rate, the rate is upper bounded by $0.5(1-\theta_N) \log_2 \left(1 + \rho_{sr,l^*}^{(max)} \right)$, where $\rho_{sr,l^*}^{(max)}$ the maximum $S \rightarrow R_l^*$ SNR for the given energy constraints.

a) *The RPSSt benchmark:* In RPSSt, the TF is split again in three phases with the first being the WPT phase. As in RHtTH and RHtT, operation during the WPT phase is described in Section II-A2. During phase II, S transmits using an MRT principle, (i.e., using as beamformer the dominant eigenvector of matrix $\mathbf{H}_{sr} \mathbf{H}_{sr}^H$). At R_{l^*} , one of the antennas, antenna m , is employing the power splitter of the system and ensures that a portion r_{ps} of the received power is fed to the EH circuit, and the remaining signal is used for communication purposes. An MRC receiver is used in order to combine the communication signal at the power splitter output with the signals at the output of the other antennas. The combiner output is forwarded during phase III, using a power level selected such as to satisfy the energy causality and energy preservation constraints.

Given that for this scheme, S transmits only for $(1+\theta)/2$, for fairness in comparison, as in RHtT, we set the power level equal to \hat{P}_s . Moreover, as for RHtTH and RHtT, we repeat the above process for all possible values of m and select the value that results in the highest achievable rate. Concerning the duration of the WPT phase, this is selected using GSS.

b) *The RtT benchmark:* RtT is obtained if the power splitter present in RPSSt is removed.

REFERENCES

- [1] S. Hu et al., "Modeling and analysis of energy harvesting and smart grid-powered wireless communication networks: A contemporary survey," *IEEE Trans. Green Commun. Netw.*, vol. 4, no. 2, pp. 461–496, Apr. 2020.
- [2] J. Wang et al., "Massive MIMO two-way relaying systems with SWIPT in IoT networks," *IEEE Internet Things J.*, vol. 8, no. 20, pp. 15 126–15 139, Aug. 2021.
- [3] B. Clerckx, Z. Popović, and R. Murch, "Future networks with wireless power transfer and energy harvesting," *Proc. IEEE*, vol. 110, no. 1, pp. 3–7, 2022.
- [4] Z. Wei et al., "Resource allocation for wireless-powered full-duplex relaying systems with nonlinear energy harvesting efficiency," *IEEE Trans. Veh. Technol.*, vol. 68, no. 12, pp. 12 079–12 093, Dec. 2019.
- [5] Ö. T. Demir and T. E. Tuncer, "Robust optimum and near-optimum beamformers for decode-and-forward full-duplex multi-antenna relay with self-energy recycling," *IEEE Trans. Wireless Commun.*, vol. 18, no. 3, pp. 1566–1580, 2019.
- [6] S. Wang, Z. He, and Y. Rong, "Joint transceiver optimization for DF multicasting MIMO relay systems with wireless information and power transfer," *IEEE Trans. Commun.*, vol. 69, no. 7, pp. 4953–4967, 2021.
- [7] A. Gupta, K. Singh, and M. Sellathurai, "Time-switching EH-based joint relay selection and resource allocation algorithms for multi-user multi-carrier AF relay networks," *IEEE Trans. Green Commun. Netw.*, vol. 3, no. 2, pp. 505–522, Mar. 2019.
- [8] Y. Ren, R. Ye, X. Zhang, S. Yang, and G. Lu, "Outage probability and throughput of wireless-powered full-duplex multi-relay systems with nonlinear EH model and imperfect CSI," in *IEEE/CIC International Conference on Communications in China (ICCC Workshops)*. IEEE, 2022, pp. 30–35.
- [9] B. Clerckx et al., "Fundamentals of wireless information and power transfer: From RF energy harvester models to signal and system designs," *IEEE J. Sel. Areas Commun.*, vol. 37, no. 1, pp. 4–33, Jan. 2019.
- [10] Y. Huang and B. Clerckx, "Waveform design for wireless power transfer with limited feedback," *IEEE Trans. Wirel. Commun.*, vol. 17, no. 1, pp. 415–429, Jan. 2018.
- [11] Y. Chen, N. Zhao, and M. Alouini, "Wireless energy harvesting using signals from multiple fading channels," *IEEE Trans. Commun.*, vol. 65, no. 11, pp. 5027–5039, Nov. 2017.
- [12] G. A. Ropokis, "Multi-relay cooperation with self-energy recycling and power consumption considerations," in *Int. Conf. on Wirel. and Mobile Comp., Netw. and Commun. (WiMob)*, Oct 2019, pp. 268–275.
- [13] Q. Gu et al., "Optimal resource allocation in wireless powered relay networks with nonlinear energy harvesters," *IEEE Wireless Commun. Lett.*, vol. 9, no. 3, pp. 371–375, 2020.

- [14] G. A. Ropokis and P. S. Bithas, "Wireless powered relay networks: Rate optimal and power consumption-aware WPT/SWIPT," *IEEE Trans. Veh. Technol.*, vol. 71, no. 8, pp. 8574–8590, Aug. 2022.
- [15] T.-T. Nguyen *et al.*, "Resource allocation for AF relaying wireless-powered networks with nonlinear energy harvester," *IEEE Commun. Lett.*, vol. 25, no. 1, pp. 229–233, Jan. 2021.
- [16] L. Shi *et al.*, "Heterogeneous power-splitting based two-way DF relaying with non-linear energy harvesting," in *IEEE Glob. Commun. Conf. (GLOBECOM)*, 2018, pp. 1–7.
- [17] M. Yang *et al.*, "Optimal time-switching relaying protocol for wireless-powered DF relay networks," in *IEEE 86th Veh. Technol. Conf. (VTC-Fall)*, 2017, pp. 1–5.
- [18] S. Kosu, M. Babaei, S. Ö. Ata, L. Durak-Ata, and H. Yanikomeroglu, "Linear/non-linear energy harvesting models via multi-antenna relay cooperation in V2V communications," *IEEE Trans. Green Commun. Netw.*, 2023.
- [19] Y. Zheng, J. Hu, and K. Yang, "Swipt aided cooperative communications with energy harvesting based selective-decode-and-forward protocol: Benefiting from channel aging effect," *IEEE Trans. Green Commun. Netw.*, 2023.
- [20] G. A. Ropokis, M. M. Butt, N. Marchetti, and L. A. DaSilva, "Optimal power allocation for energy recycling assisted cooperative communications," in *IEEE Wireless Commun. and Netw. Conf. Workshops (WCNCW)*, Mar. 2017, pp. 1–6.
- [21] G. A. Ropokis, N. Marchetti, and L. A. DaSilva, "Cooperative beamforming exploiting energy recycling," in *25th Int. Conf. on Telecommun. (ICT)*, June 2018, pp. 577–582.
- [22] K. Kwon, D. Hwang, and S. S. Nam, "Beamformer design for self-energy recycling in full-duplex decode-and-forward relay systems," *IEEE Wirel. Commun.*, vol. 9, no. 9, pp. 1417–1421, Sep. 2020.
- [23] K. Kwon, D. Hwang, H.-K. Song, and S. S. Nam, "Full-duplex with self-energy recycling in the RF powered multi-antenna relay channels," *IEEE Signal Process. Lett.*, vol. 26, no. 10, pp. 1516–1520, Oct. 2019.
- [24] D. N. K. Jayakody *et al.*, "Self-energized UAV-assisted scheme for cooperative wireless relay networks," *IEEE Trans. on Veh. Technol.*, vol. 69, no. 1, pp. 578–592, Jan. 2020.
- [25] O. T. Demir and T. E. Tuncer, "Robust optimum and near-optimum beamformers for decode-and-forward full-duplex multi-antenna relay with self-energy recycling," *IEEE Trans. Wireless Comm.*, no. 3, pp. 1566–1580, Mar. 2019.
- [26] Y. Zeng and R. Zhang, "Full-duplex wireless-powered relay with self-energy recycling," *IEEE Wireless Commun. Lett.*, vol. 4, no. 2, pp. 201–204, April 2015.
- [27] S. Rajan *et al.*, "Efficient approximations for the arctangent function," *IEEE Signal Process. Mag.*, vol. 23, no. 3, pp. 108–111, 2006.
- [28] S. Zarei, W. H. Gerstacker, R. Weigel, M. Vossiek, and R. Schober, "Robust MSE-balancing hierarchical linear/Tomlinson-Harashima precoding for downlink massive MU-MIMO systems," *IEEE Trans. Wireless Commun.*, vol. 17, no. 11, pp. 7309–7324, 2018.
- [29] E. Boshkovska *et al.*, "Secure SWIPT networks based on a non-linear energy harvesting model," in *IEEE Wireless Communications and Networking Conference Workshops (WCNCW)*, 2017, pp. 1–6.
- [30] C. Zhai, L. Zheng, P. Lan, and H. Chen, "Wireless powered cooperative communication using two relays: Protocol design and performance analysis," *IEEE Trans. on Veh. Technol.*, vol. 67, no. 4, pp. 3598–3611, 2018.
- [31] Y. Liu, Q. Chen, and L. X. Cai, "Throughput maximization for wireless powered buffer-aided successive relaying networks," *Wireless Communications and Mobile Computing*, vol. Article ID 4258113, 2022.
- [32] Z. Q. Luo *et al.*, "Semidefinite relaxation of quadratic optimization problems," *IEEE Signal Process. Mag.*, vol. 27, no. 3, pp. 20–34, May 2010.
- [33] G. Pataki, "On the rank of extreme matrices in semidefinite programs and the multiplicity of optimal eigenvalues," *Mathematics of Operations Research*, vol. 23, no. 2, pp. 339–358, 1998.



George A. Ropokis is an Associate Professor at CentraleSupélec, Campus Rennes, also affiliated with the Institute of Electronics and Telecommunications of Rennes. He received the Diploma degree in Computer Engineering and Informatics from the Univ. of Patras, Greece in 2004, the M.Sc. degree in Mobile and Satellite Communications from the Univ. of Surrey, U.K. and the Ph.D. degree in Wireless Communications from the Univ. of Patras in 2010. From 2012 to 2014 he was a Visiting Scientist at the Mobile Comm. Dept., EURECOM, France. From 2016 to 2018, he served as a Research Fellow at CONNECT centre, Trinity College Dublin, Ireland. His research interests are focused on the performance analysis and optimization of Wireless Communications systems.



Petros S. Bithas (S'04-M'09-SM'19) received the Diploma in electrical and computer engineering and PhD degree, from the Univ. of Patras, Greece, in 2003 and 2009, respectively. During 2009–2018 he was with the Department of Electronic Engineering of the Technological Educational Institute of Piraeus, Greece. He is currently an Associate Professor at the Department of Digital Industry Technologies of the National & Kapodistrian University of Athens, Greece. He serves on the Editorial Board of the *IEEE Communication Letters*. His research interests include stochastic modeling of wireless communication systems.